Physicochemical Studies of Fluorescent Dyes Doped in Polymer Sheet and Its Application in Solar Energy: Effect of Gamma Irradiation on Charge–Transfer Complex of 1,8-naphthalimide Derivative with Chloranilic Acid

M.S. Al-Amoudi[1], H.E. Hassan[2,3], M.M. AL-Majthoub[1], T. Sharshar[2,4], Moamen S. Refat[1,5],*

[1] Chemistry Department, Faculty of Science, Taif University, P.O. Box 888, Al-Hawiah, Taif 21974, Saudi Arabia
[2] Physics Department, Faculty of Science, Taif University, P.O. Box 888, Al-Hawiah, Taif 21974, Saudi Arabia
[3] Cyclotron Facility, Nuclear Research Center, Atomic Energy Authority, Cairo 13759, Egypt
[4] Physics Department, Faculty of Science, Kafrelsheikh University, Kafr El-Sheikh, Egypt
[5] Chemistry Department, Faculty of Science, Port Said University, Port Said, Egypt
[*]E-mail: dr_alamoudi@yahoo.com

Charge-transfer complex formed from the reaction of 2-(4-isobutoxyphenyl)-6-hydrazino-1,8-naphthalimide dye with chloranilic acid (CLA) has been studied in methanol at room temperature. The final reaction product has been isolated and characterized using UV-Vis. and infrared spectra. The thermal stability measurements (TG/DTG) as well as elemental analysis of carbon, hydrogen and nitrogen elements were also performed for this sample. The photometric titration curves for the reaction indicated that the data obtained refer to 1:2 (CLA:dye) charge transfer complex $[(nap)_2(CLA)]$ was formed. The activation parameters ΔE, ΔH, ΔS and ΔG were obtained from the DTG diagrams by using Coats-Redfern method. The infrared spectra interpreted the mode of charge–transfer interaction associated with the hydrogen bonding exist between a two protons (–OH) of phenolic groups of CLA acidic central positions of acceptors and the terminal amino group for two dye moieties. Gamma irradiation was tested as a method for stabilization of fluorescent dyes doped in polymer sheets. The effect of gamma irradiation of 70 kGy dose on the properties of the charge transfer was studied using different techniques such as photolumencies (PL) and positron annihilation spectroscopy. The positron annihilation lifetime parameters and the doppler broadening line-shape S parameter were found to be dependent on the structure, electronic configuration the charge transfer complex. The positron annihilation spectroscopy can be used as a probe to study the stability of the fluorescent dyes.

1. INTRODUCTION

The study of structure stability of dyes and polymer matrices have been given a great deal of attention for many years, which leads to enhancing the prospects of sensors [1–4], energy storage [5,6], solar energy conversion [7-12]. The charge transfer complexes formed during the reaction of fluorescent dyes as a donor or electron acceptor play important role in synthesis of the fluorescent dyes and choice of their applications [13,14]. The solar energy is clean and non hazardous, could contribute considerably to a solution of the energy problems if appropriate methods could be developed to collect, concentrate, store, and convert solar radiation [1]. Fluorescent solar collectors (FSCs) gained a lot of attention since the first proposal owned by Weber and Lambe [15]. In recent years, sol-gel technique has been extensively used to prepare the organic dyes doped into inorganic host matrix which found potentials in optical applications [16]. The using of sol gel technique to prepare glass matrix of fluorescent dyes has the advantages of low cost and applying low temperature which prevent thermal degradation. One of these matrices is   N, N′-bis-substituted-1,4,6,8-naphthalene-diimides which have been investigated intensively because of their promising applications. It can be used in solar energy collectors [17], electronic and molecular devises [18, 19], DNA sensors [20] or antibacterial agents [21, 22] and photoactive materials [23, 24]. The quenching effect on the fluorescence intensity of N,N′-bis-substituted-1,4,6,8-naphthalenediimides have been investigated [25, 26]. A systematic quantitative study of the solubility of various naphthalene-diimides in organic solvents with different polarity has been investigated by means of UV-Vis spectroscopy [27]. This study showed the results obtained from the electronic, infrared, fluorescence efficiency and thermal gravimetric measurements as well as the kinetic thermodynamic parameters calculated on 2-(4-isobutoxyphenyl)-6-hydrazino-1,8-naphthalimide dye (nap) and its chloranilic acid complex in powder and polymeric sheet form. From this study it is expected that the donor contains terminal amino group within hydrazine moiety, which cause increasing in the stability of the resulted complex.

The aim of this work is to perform assessments of the photostability of the 1,8-naphthalimide dye by operated charge–transfer reaction with chloranilic acid acceptor in the form of powder and polymeric sheets. The stiochiometry and the interaction mode resulted from the charge–transfer complex and their effects on the fluorescence efficiency and thermal stability behaviors of the $[(nap)_2(CLA)]$ charge–transfer adduct will be investigated. The determination of association constant (K), molar extinction coefficients (ε) and oscillator strength (f) is carried out. From previously reported studies, it was shown that the properties of polymers are very sensitive to ionizing radiation. It is already an established fact that interaction of radiation with polymers leads to chain scission, chain aggregation, formation of double bonds and molecular emission. As a consequence of this, the physico-chemical properties like optical, electrical, mechanical, chemical and track properties of the polymer are modified [28,29]. The effectiveness of these changes produced depends upon the structure of the polymer and the experimental conditions of irradiation like energy and fluency. The study of these changes may enhance their applications in doesimetric applications [30], e.g. for the evolution of high radiation doses [31]. Therefore, we extend our study in this work to the investigation of γ-rays irradiation effects on the physicochemical properties of the studies $[(nap)_2(CLA)]$ complex. The

Positron annihilation spectroscopy will be used as an accurate tool for identifying the changes in the structure due to formation of the complex and γ-rays irradiation effects.

2. EXPERIMENTAL

2.1 Materials
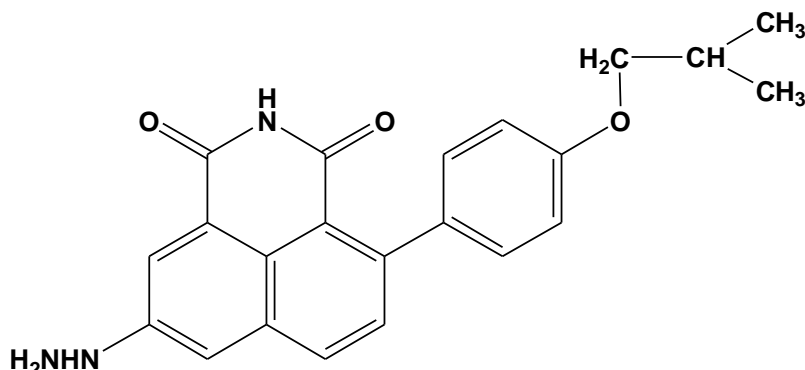
Figure 1. Structure of 2-(4-isobutoxyphenyl)-6-hydrazino-1,8-naphthalimide dye

All chemicals and solvents (methylene chloride; CH_2Cl_2 and dimethylsulfoxide DMSO) used were of fine grade. The 2-(4-isobutoxyphenyl)-6-hydrazino-1,8-naphthalimide dye (nap; Fig. 1) (MF= $C_{22}H_{21}N_3O_3$/Mwt= 375.42 g/mol) were obtained from Institute of Polymers, Bulgarian Academy of Science and were used without further purification. The chloranilic acid; CLA and Poly(methyl methacrylate) (PMMA) were purchased from Merck Chemical Company and were also used as received. All solvents (methylene chloride; CH_2Cl_2 and dimethylsulfoxide; DMSO) pursed from Fluka, Merck were highly pure of spectroscopic grade.

2.2 Synthetic solid powder of [(nap)₂(CLA)] charge–transfer adduct

The solid charge–transfer product of nap and CLA was synthesized by mixing 2 mmol-to-1 mmol amounts of (nap: CLA) in 50 mL of methylene chloride. The mixtures were stirred for 45 min, and allowed to evaporate slowly at room temperature, which resulted in the precipitation of the solid charge–transfer complex. The separated complex was filtered off, washed well with little amounts of methylene chloride, and then collected and dried under vacuum over anhydrous calcium chloride for 48 h.

2.3 Preparation of dyed polymer sheet

Both Poly(methyl methacrylate) (PMMA) grains and dye or its chloranilic acid complex was dissolved in methylene chloride and mixed using a magnetic stirrer. The homogenous mixture was poured into a glass petri dish and allowed to dry (Scheme 1).

Scheme 1. Photos of the prepared sheets of Polymethyl methacrylate (PMMA): (A) blanck sheet (B) doped by nap (C) doped by nap-CLA

2.4 Photometric titration

The photometric titration measurements were carried out for the reaction of nap with CLA against methanol as a blank at wavelength 449 nm. A 0.25, 0.50, 0.75, 1.00, 1.50, 2.0, 2.50, 3.00, 3.50 or 4.00 mL aliquot of a standard solution (5.0×10^{-4} M) of the nap dye donor in MeOH was added to 1.00 ml (5.0×10^{-4} M) of CLA acceptor, which was also dissolved in MeOH. The total volume of the mixture was 5 mL. The concentration of the donors (C_d) in the reaction mixture was maintained at 5.0×10^{-4} M, whereas the concentration of the acceptor (C_a) changed over a wide range of concentrations (0.25×10^{-4} - 4.00×10^{-4} M) to produce solutions with an acceptor molar ratio that varied from 4:1 to 1:4. The stoichiometry of the molecular CT complex was obtained from the determination of the conventional spectrophotometric molar ratio according to known methods [32] using a plot of the absorbance of each CT complex as a function of the C_d:C_a ratio. Modified Benesi–Hildebrand plots [33, 34] were constructed to allow the calculation of the formation constant, K_{CT}, and the absorptivity, ε_{CT}, values for charge-transfer complex in this study.

2.5 Instrumentation

The elemental analyses of the carbon, hydrogen and nitrogen contents were performed using a Perkin-Elmer CHN 2400 (USA). The electronic absorption spectra of methanolic solutions of the donor, acceptor and resulting CT complex were recorded over a wavelength range of 200-800 nm using a UV/Vis double-beam JASCO-V-670 spectrophotometer. The instrument was equipped with a quartz cell with a 1.0 cm path length. The molar conductivities of freshly prepared 1.0×10^{-3} mol/cm^3 dimethylsulfoxide (DMSO) solutions were measured for the dissolved free dye and its charge-transfer complex using Jenway 4010 conductivity meter. The mid-infrared (IR) spectra (KBr discs) within the range of 4000-400 cm^{-1} for the solid powder and polymer sheets of free dye and its charge-transfer complex were recorded on a Bruker FT-IR spectrophotometer with 30 scans at 2 cm^{-1} resolution. Thermogravimetric analysis (TG/DTG) was performed under static nitrogen atmosphere between room temperature and 800 °C at a heating rate of 10 °C/min using a Shimadzu TGA–50H thermal analyzer. Steady state emission spectra were measured with a FluoroMax®-4 Spectrofluorometer-Horiba Scientific using rectangular quartz cell of dimensions 0.2 cm x 1 cm to minimize re–absorption effect.

A group of the prepared samples (assigned PMMA polymer, nap and nap-CLA) was irradiated by γ rays of ^{60}Co radioactive source at room temperature using irradiation cell (medical sterilizer type

CM-20) in the cyclotron facility, Nuclear Research Center, Atomic Energy Authority, Cairo, Egypt. The total exposure dose was 70 kGy with dose rate 1.46 kGy/h. The irradiated samples were assigned with PMMA-D1, nap-D1 and nap-CLA-D1. All samples were measured using the above mentioned techniques to study the effect of γ irradiation on their properties.

The PAL measurements were carried out using a fast-fast coincidence spectrometer [35]. This PAL spectrometer consists of two Bicron BC-418 plastic scintillation detectors, and Ortec modules; two 583 constant fraction differential discriminators (CFDD), DB643 delay box (ns D), 414A fast coincidence and 566 time-to-amplitude converter (TAC). The data were acquired using an Ortec 919 multichannel analyzer (MCA). A positron source was prepared using a droplet of ^{22}NaCl solution dried onto two identical Kapton foils (7.5 μm thick), which were afterward glued by epoxy glue. This source was sandwiched between two identical samples. The lifetime spectra were measured in air at room temperature. More than one million counts were accumulated for each spectrum and each sample was measured three times. The time resolution of the spectrometer, measured with ^{60}Co source at ^{22}Na energy window settings, was ~310 ps (full-width at half maximum). The positron annihilation lifetime is measured experimentally as the time interval between the 1274.5 keV γ ray emitted by the ^{22}Na radioisotope and one of the annihilation radiations. The resulting lifetime spectra were analyzed using a computer program LT with a suitable correction for positrons annihilated in the Kapton [36].

When injected into molecular solids, positrons can form positronium (Ps), which is the bound state of an electron and a positron: para-positronium (p-Ps) in which the positron and the electron have opposite spins and ortho-positronium (o-Ps) in which the spins are parallel. In general, if Ps is formed, the experimental lifetime spectra consist of three exponential components representing p-Ps (τ_1 = 125 ps) free and bound positrons (τ_2 = 150-500 ps) and o-Ps (τ_3 > 900 ps), with the associated formation probabilities I_1, I_2 and I_3, respectively. The time resolution of the spectrometer (~310 ps) makes the data on the shortest-lived component ascribed to p-Ps somewhat unreliable. Thererfore, τ_1 was fixed at 125 ps to reduce the scatter of the other parameters. All exponential components of the measured lifetime spectra were determined with the best-fitting parameter ranged from 0.99 to 1.1. The range of the experimental errors for the PAL parameters τ_2, τ_3, I_1, I_2 and I_3, determined over multiple measurements, were found to be <2.9 ps, <18 ps, 1.4%, 1.2% and 0.4%, respectively. The mean lifetime of positron is direct proportional to the average defect density. It was calculated using the following relation:

$$\tau_m = \frac{\tau_1 I_1 + \tau_2 I_2 + \tau_3 I_3}{I_1 + I_2 + I_3} \qquad (1)$$

The mean free volume, V_f (in nm^3), can be calculated by a simple relation given below, assuming a spherical shape for the holes [37,38]: $V_f = 4/3 \ \pi R^3$ where R (nm) is the average radius of the free volume hole. R is determined using a semiempirical equation with the values of τ_3 [39,40]. Furthermore, the free volume hole fraction, *fv*, can be found from the empirical equation [41, 42]:

$$f_v = C V_f I_3, \qquad (2)$$

where V_f is in Å^3, I_3 in %, and C is an arbitrarily chosen scaling factor for a spherical cavity.

The Doppler broadening line shape S-parameter was measured using a p-type high-purity germanium detector (Ortec, GEM series) with an energy resolution (FWHM) of 1.6 keV for 1.33 MeV gamma line of ^{60}Co and relative efficiency of 25%. The amplified signals from an Ortec 570 amplifier

were acquired with the Ortec 919 MCA. The ^{133}Ba source was used for energy calibration (68 eV/channel). Samples spectra were collected for 120 min. The S–parameter is more sensitive to the annihilation with low momentum valence and unbound electrons. The S–parameter is defined as the ratio of the integration over the central part of the annihilation line to the total integration. The Doppler broadening Spectra were analyzed using SP ver. 1.0 program [43]. The most important is to determine the channel with maximum counts that corresponds to the energy 511 keV. Defining the maximum counts is necessary because it is a base for calculations of S–parameter. The channel numbers (input data) for this program are fixed for all measurements.

3. RESULTS AND DISCUSSION

3.1 Physicochemical studies of fluorescent dye complex in solid powder form

3.1.1 Elemental analyses results

The analytical data of the elemental analysis of the nap/CLA charge–transfer complex are as follows: [(nap)$_2$(CLA)]; $C_{50}H_{44}N_6Cl_2O_{10}$: M.wt. = 959.82 g/mol; Calc.: %C, 62.57; %H, 4.62; %N, 8.76, Found: %C, 62.32; %H, 4.49; %N, 8.61. The resulting values are in good agreement with the calculated values, and the suggested values are in agreement with the molar ratios determined from the photometric titration curve. The stoichiometry of the nap/CLA charge–transfer complex was found to be 2:1 ratios. Based on the obtained data, the formed charge–transfer complex was formulated as [(nap)$_2$(CLA)]. Molar conductance of the [(nap)$_2$(CLA)] charge–transfer complex in DMSO solvent at 10^{-3} molar concentrations were obtained in the range 50 $\Omega^{-1}cm^2mol^{-1}$ and this result indicated that the formed CT complex is a weak electrolyte. This result established the stoichiometry of this complex, which is in agreement with the general formula, was suggested.

3.1.2 Electronic absorption spectra

Fig. 2 shows the electronic absorption spectra of the nap, CLA, and the formed charge–transfer complex, these spectra revealed a new absorption band at 449 nm that is attributed to the CT donor-acceptor interaction, [(nap)$_2$(CLA)] complex. This peak absorbance values that appeared in the electronic spectra assigned to the formed CT complex is plotted as function of the C_d: C_a ratio according to the known method [33]. The photometric titration curve of the CT complex is given in Fig. 3, which confirmed that the complex was formed at a ratio 2:1 (nap: acceptor). The formation constant (K_{CT}) and the molar absorptivity (ε) of this complex was calculated by applying the 1:2 modified Benesi–Hildebrand equation (3) [33, 34]:

$$(C_a)^2 C_d/A = 1/K\varepsilon + 1/\varepsilon\, C_a(4C_d + C_a) \qquad (3)$$

where C_a and C_d are the initial concentrations of the acceptor and the donor, respectively, and A is the absorbance of the strongly detected CT band.
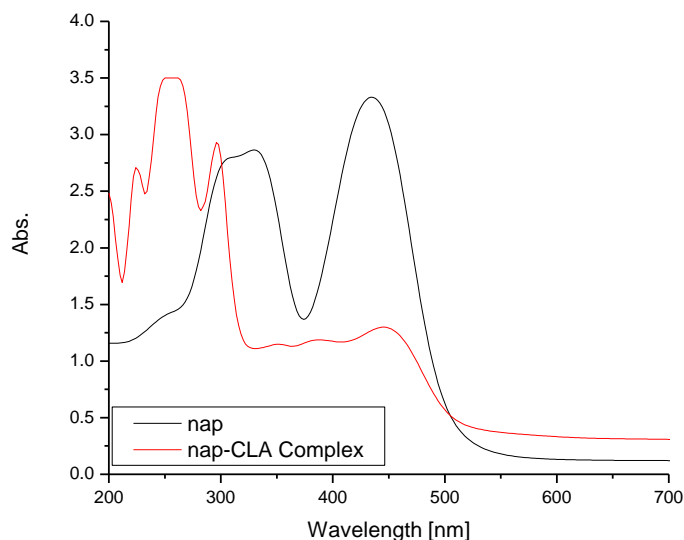
Figure 2. Electronic absorption spectra of 2-(4-isobutoxyphenyl)-6-hydrazino-1,8-naphthalimide dye charge–transfer complex.
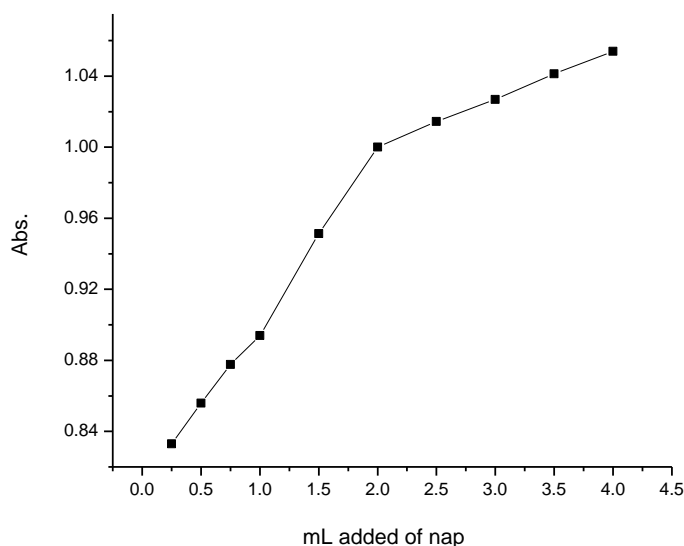
Figure 3. Photometric titration curves for nap/CLA charge–transfer complex

Plotting $(C_a)^2 C_d / A$ values versus the corresponding $C_a(4C_d + C_a)$ values for the formed charge-transfer complex, straight line are obtained supporting our finding of the formation of 1:2 complexes (see Fig. 4). In the plots, the slope and intercept equal $1/\varepsilon$ and $1/K\varepsilon$, respectively. The modified Benesi–Hildebrand plots are shown in Fig. 4. The values of both K_{CT} and ε associated with the complex are given in Table 1. This complex exhibit high values of both the formation constant (K_{CT}) and the extinction coefficients (ε). The high value of K_{CT} reflects highly stability of the formed charge–transfer complex. The data reveal that the $[(nap)_2(CLA)]$ complex shows a higher K_{CT} value which assigned to the relatively higher powerful electron acceptance ability (withdrawing groups) for CLA acceptor.

Table 1. Spectrophotometric results of the nap/CLA charge–transfer complex

Complex	CT-absorption (nm)	E_{CT} (eV)	K (Lmol^{-1})	ε_{max} (Lmol^{-1}cm^{-1})	f	μ	I_p	R_N	$\Delta G°$ (25 °C) (kJmol^{-1})
[(nap)(CLA)]	449	2.77	4×10^7	2×10^4	4.32	61	9.17	0.377	-44.763
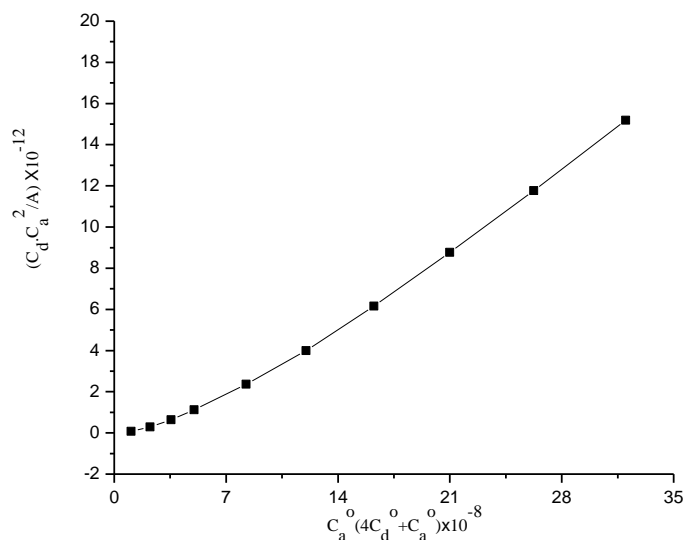
Figure 4. The modified Benesi-Hildebrand plot of nap/CLA charge–transfer complex

3.1.3 Calculation of the spectroscopic and physical data

The spectroscopic and physical data, such as the standard free energy ($\Delta G°$), the oscillator strength (f), the transition dipole moment (μ), the resonance energy (R_N), and the ionization potential (I_P), were estimated for nap/CLA system dissolved in methanol at 25 °C. The calculations can be summarized as follow:

The oscillator strength (f) is a dimensionless quantity used to express the transition probability of the charge–transfer band From the CT absorption spectra [44], and can be estimated using the approximate formula [45]:

$$f = 4.319\times10^{-9} \int \varepsilon_{CT}\, dv \qquad (4)$$

where $\int \varepsilon_{CT}\, dv$ is the area under the curve of the extinction coefficient of the absorption band in question plotted as a function of frequency. To a first approximation,

$$f = 4.319\times10^{-9}\, \varepsilon_{CT} v_{\frac{1}{2}} \qquad (5)$$

where ε_{CT} is the maximum extinction coefficient of the charge–transfer band, and $v_{\frac{1}{2}}$ is the half-bandwidth in cm^{-1} (i.e., the width of the band at half the maximum extinction). The transition dipole moments (μ) of the CT complex has been calculated from Eq. (6) [46]:

$$\mu = 0.0958\, [\varepsilon_{CT} v_{\frac{1}{2}} / v_{max}]^{\frac{1}{2}} \qquad (6)$$

The transition dipole moment can be used to determine if a particular transition is allowed; the transition from a bonding π orbital to an antibonding π^* orbital is allowed because the integral that

defines the transition dipole moment is nonzero. The ionization potential (I_P) of the dye donor in the charge–transfer complex was calculated using the empirical equation derived by Aloisi and Pignataro represented in Eq. (6) [47]:

$$I_P (eV) = 5.76 + 1.53 \times 10^{-4} \nu_{CT} \qquad (7)$$

where ν_{CT} is the wavenumber in cm^{-1} that corresponds to the charge–transfer band formed from the interaction between the donor and the acceptor. The electron-donating power of a donor molecule is measured by its ionization potential, which is the energy required to remove an electron from the highest occupied molecular orbital. Briegleb and Czekalla [48] theoretically derived the following relationship to obtain the resonance energy (R_N):

$$\varepsilon_{CT} = 7.7 \times 10^{-4} / [h\nu_{CT}/[R_N]\text{-}3.5] \qquad (8)$$

where ε_{CT} is the molar absorptivity coefficient of the CT complex at the maximum of the CT absorption, ν_{CT} is the frequency of the CT peak, and R_N is the resonance energy of the complex in the ground state, which contributes to the stability constant of the complex (a ground-state property). The energy values (E_{CT}) of the n→π^* and π–π^* interactions between the donor and the acceptor were calculated using the equation derived by Briegleb [49]:

$$E_{CT} = (h\nu_{CT}) = (1243.667/\lambda_{CT}) \qquad (9)$$

where λ_{CT} is the wavelength of the CT band of the formed complex. The standard free energy of complexation ($\Delta G°$) for the complex was calculated from the formation constants using the equation derived by Martin et al. [50]:

$$\Delta G° = \text{-}2.303RT \log K_{CT} \qquad (10)$$

where $\Delta G°$ is the free energy change of the CT complex (kJmol^{-1}), R is the gas constant (8.314 Jmol^{-1}K), T is the absolute temperature in K, and K_{CT} is the formation constant of the complex (Lmol^{-1}) at room temperature.

The calculated spectroscopic and physical values (f, μ, I_P, R_N and $\Delta G°$) for the nap charge–transfer complex using these equations are presented in Table 1. [(nap)$_2$(CLA)] complex exhibits higher values of both the oscillator strength (f) and the transition dipole moment (μ). Chloranilic acid is a strong electron acceptor to form stable CT complexes with the donors. Beside this function, CLA is a strong acid (pK$_a$=2.95 and 4.97) [51], hence a proton transfer from CLA to the donors is expected. The observed high values of f indicate a strong interaction between the donor–acceptor pairs with relatively high probabilities of charge–transfer transitions [52]. One important aspect of characterizing charge–transfer complexes is the calculation of the ionization potential (I_P) of the donor. The calculated I_P value for the highest filled molecular orbital that participates in the charge–transfer interaction of the nap is approximately 9.17 eV. The ionization potential of the electron donor has been reported to be correlated with the charge–transfer transition energy of the complex [53]. Further evidence for the nature of charge–transfer interactions is the calculation of the standard free energy change ($\Delta G°$). The obtained values of $\Delta G°$ for the nap/CLA complex is –44.763 kJmol^{-1}, this negative value indicate that the interaction between nap and the CLA acceptor is spontaneous [54, 55]. In general, $\Delta G°$ values are more negative as the formation constants of the charge–transfer complexes increase. As the bond between the donor and acceptor becomes stronger and thus the components are subjected to more physical strain or loss freedom, the values of $\Delta G°$ become more negative. It is seen

that higher the HOMO-LUMO energy gap, higher is the acceptor affinity and hence stability of complex.

3.1.4 Infrared spectra
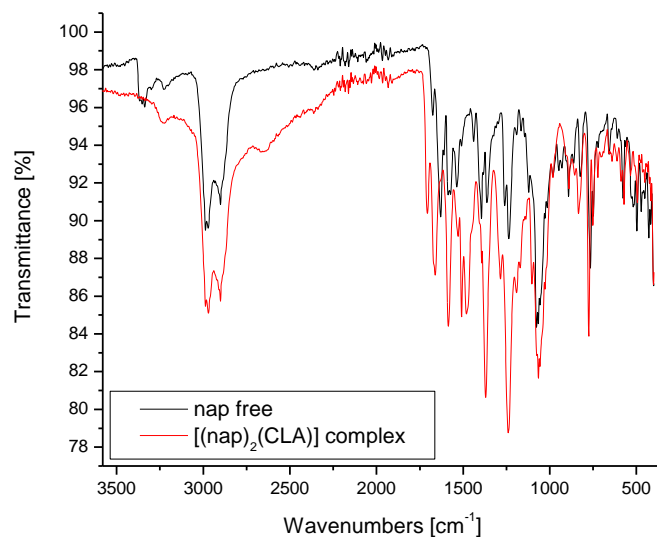
Figure 5. Infrared spectra of nap free donor and its CLA charge–transfer complex
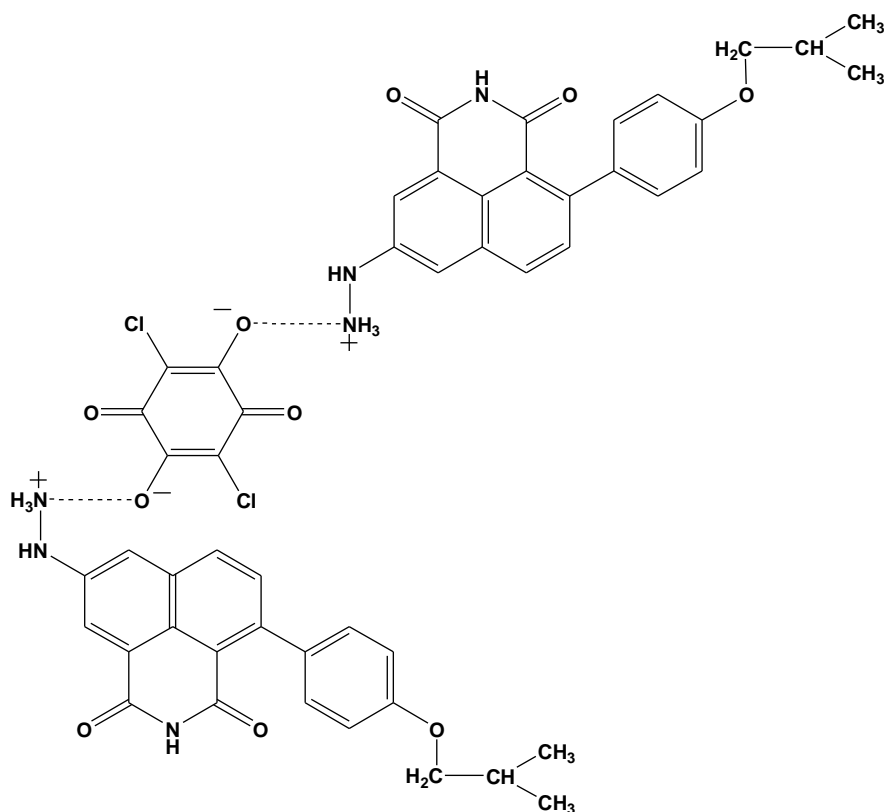
Figure 6. Suggested structure of [(nap)$_2$(CLA)] charge–transfer complex

Table 2. Infrared frequencies (cm^{-1}) and tentative assignments for CLA, nap and [(Pon)(CLA)$_2$] charge–transfer complex

CLA	nap	nap/CLA	Assignments
3235	-- 3354	--	ν(O-H); CLA ν(N-H); NH$_2$ hydrazino group
--	3229	3230	ν(N-H); NH hydrazino group
--	2980, 2897	2972, 2897	ν_s(C-H) + ν_{as}(C-H); aliphatic and aromatic groups
--	--	2648	Intermolecular hydrogen bonding
1664, 1630	1676	1708, 1663	ν(C=O); amido group of nap + keto group of CLA
	1626 1580	-- 1587	δ(NH$_2$); amido group of nap δ(NH); amido group of nap
	1539, 1509, 1441,1396	1531, 1509, 1482	ν(C=C); ph
1368, 1263, 1207, 1168	1362, 1261, 1239, 1126 1069	1374, 1287, 1238, 1107, 1066	C-H deformation ν(C-C) + ν(C-N) + ν(C-O)
981, 851	893, 821	893, 836	(C-H) bend ν(C-Cl); CLA
752, 690, 569	765, 659, 578, 495	776, 570, 495	Skeletal vibrations CNC deformation

The mid infrared spectra of 2-(4-isobutoxyphenyl)-6-hydrazino-1,8-naphthalimide free dye and the resulted charge–transfer complex of [(nap)$_2$(CLA)] were recorded from KBr discs. These spectra are shown in Fig. 5. The infrared spectral bands are resolved and assigned into their vibrational modes and given in Table 2. The absence of ν(O–H) at 3235 cm^{-1} for chloranilic acid acceptor and (ν(NH$_2$) and δ(NH$_2$)) at 3354 and 1626 cm^{-1} for (hydrazine group), respectively, clearly indicates that charge–transfer interaction associated with the hydrogen bonding exist between a two acidic protons (–OH) of chloranilic acid acceptor and two nap moieties of donor. The presence of bands at 3230 and 1587 cm^{-1} are due to ν(NH$_2$) and δ(NH$_2$), respectively, [56] assigned to unsharing of –NH group for both hydrazino and amido moieties in the complexation. The results indicate that the nap shows a noticeable shift in the intensities and higher wavenumbers for the ν(C=O) vibration bands due to the chelation of C=O is faraway the intermolecular hydrogen bond. In [(nap)(CLA)$_2$] complex, the band at 2684 cm^{-1} is assigned to the stretching vibration motion of intermolecular hydrogen bond, which indicate the binding of both –OH (chloranilic acid) toward NH$_2$ (nap donor dye) to form $^+$NH$_3$ group. As expected, the bands characteristic for the nap unit in [(nap)$_2$(CLA)] are shown with small changes in band intensities values of aromatic rings groups upon the electronic configuration. The mode of interaction between nap and chloranilic acid acceptor can be presented as shown in Fig. 6.

3.1.5 Thermal analysis
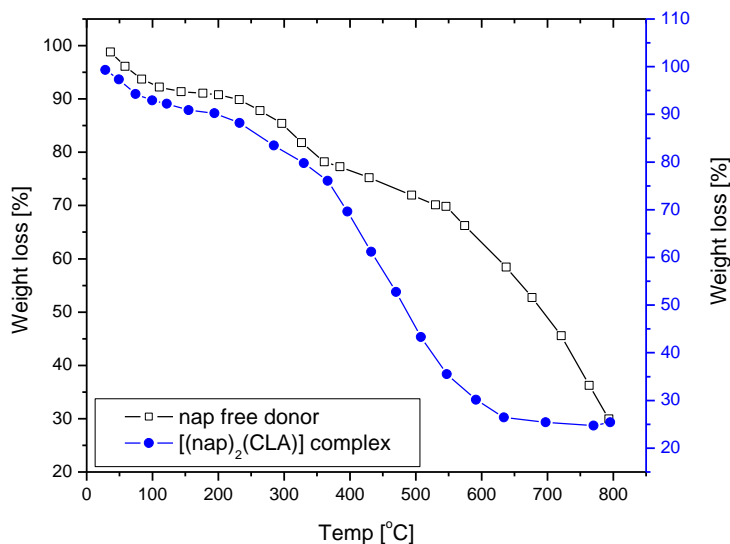
Figure 7a. TG diagrams of nap free donor and its CLA charge–transfer complex
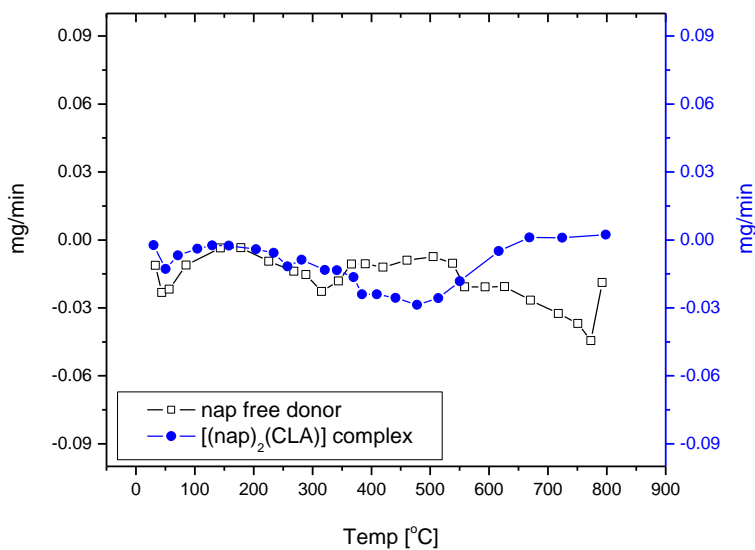
Figure 7b. DTG diagrams of nap free donor and its CLA charge–transfer complex

The characteristic temperatures for the thermal decomposition (TG/DTG) of the studied charge–transfer complex of nap and $[(nap)_2(CLA)]$ are presented in Fig. 7a-b, the following steps discussed the decomposition stages occur in the three decomposition steps. The thermogram for the nap free donor show three degradation steps at DTG_{max}= 53, 315 and 773 ^{o}C with a weight losses of 74% dealing with the loss of $C_{14}H_{21}N_3O_3$. The residual of degradation mechanism is assigned to few carbon atoms. The thermogram for $[(nap)_2(CLA)]$, shows three decomposition steps at 50, 256 and 472 ^{o}C with a weight losses of about 75% correspond to the loss of two CLA and two nap molecules and

also remaining 25% of few carbon atoms. The physical results (melting points of reactants and products are difference) clearly indicate that the reaction products seem newly charge-transfer compound that has a chemical and physical behavior than reactants.

3.1.6 Kinetic studies

Table 3. Kinetic thermodynamic data of nap and [(nap)(CLA)$_2$] charge–transfer complex

Complexes	DTG$_{max}$/^{o}C	ΔE kJmol^{-1}	ΔH kJmol^{-1}	ΔS Jmol^{-1}K^{-1}	ΔG kJmol^{-1}	r
Nap	315	935	89	-144	175	0.9960
[(nap)$_2$(CLA)]	472	79	75	-151	155	0.9902

The influence of the type of acceptors on the stability of the resulted charge–transfer complex can be investigated kinetically using the Coats-Redfern method equation (9) [57]. The data are listed in Table 3. The thermodynamic data was applied on the main decomposition peaks at 315 and 472 ^{o}C for nap and [(nap)(CLA)$_2$] charge–transfer complex, respectively.

$$\ln\left[\frac{-\ln(1-\alpha)}{T^2}\right] = \ln\left(\frac{ZR}{\varphi E}\right) - \frac{E}{RT} \qquad (11)$$

Where α, and φ are the fraction of the sample decomposed at time t and the linear heating rate, respectively. R is the gas constant and E is the activation energy in kJ mol^{-1}.

A plot of $\ln\left[\frac{-\ln(1-\alpha)}{T^2}\right]$ against $1/T$ was found to be linear from the slope of which E, was calculated and Z (Arrhenius constant) can be deduced from the intercept. The enthalpy of activation, ΔH, and the free enthalpy of activation, ΔG, can be calculated (Table 3) via the following equation (10);

$$\Delta H = E - RT_m \ ; \ \Delta G = \Delta H - T_m \Delta S \qquad (12)$$

Accordingly, the kinetic data in Table 3, the charge–transfer complex has −ve entropy, which indicates that activated complex has more ordered system than reactants. In Table 3, it was found that the [(nap)$_2$(CLA)] complex has a higher thermal stability, because of the CLA acceptor has an electron withdrawing group (two chloro and two carbonyl groups) make more facility to charge–transfer complexation.

3.2 Physicochemical studies of fluorescent dye complex in polymer sheet form

3.2.1 Infrared spectra studies

The infrared spectra confirm the physical feature of the composites. The infrared spectral bands of superimposition of compositions can be seen in Fig. 8. Physical nature of the PMMA (blank polymer sheet before and after irradiation), nap free dye (before and after irradiation) and charge

transfer complex [(nap)$_2$(CLA)] (before and after irradiation) composites were checked using assignments of infrared spectral bands.
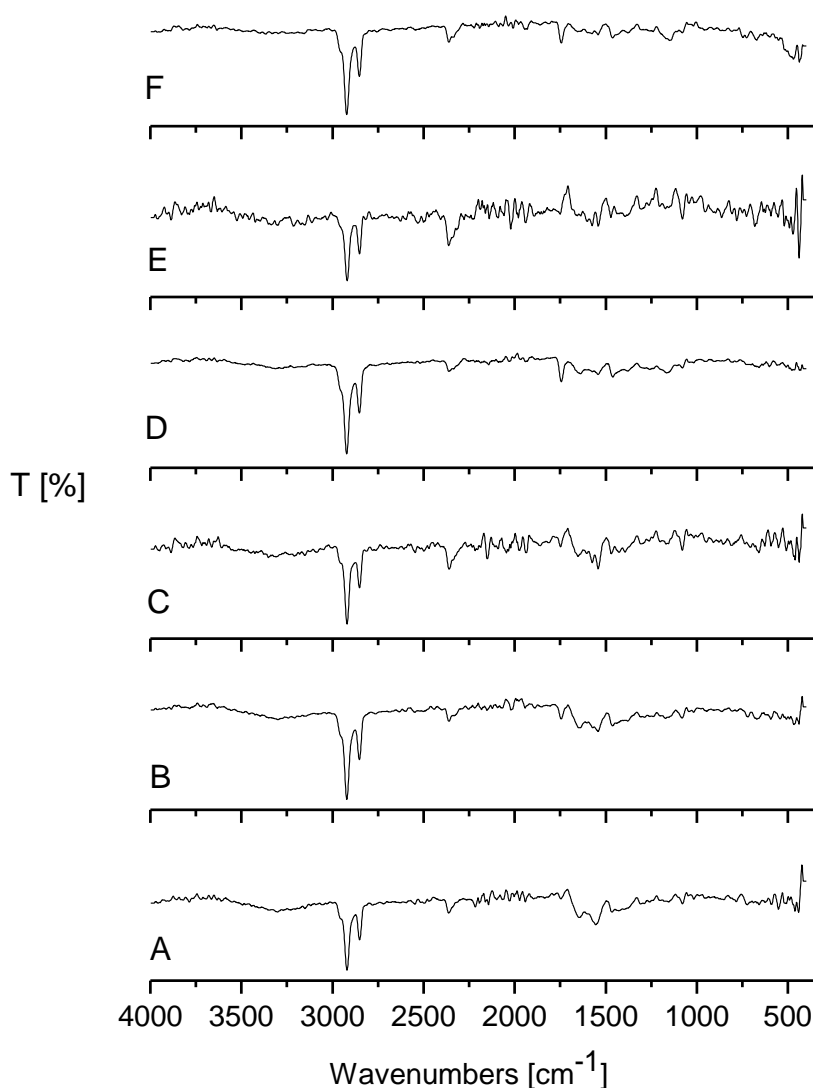
Figure 8. Infrared spectra of polymeric sheets for (A): PMMA (before Irr.), (B): PMMA (after Irr.), (C): PMMA-nap (before Irr.), (D): PMMA-nap (after Irr.), (E): PMMA-nap-CLA (before Irr.) and (F): PMMA-nap-CLA (after Irr.).

The defined frequencies data have shown the superimposition of reactant materials. For example, the infrared spectra of PMMA, nap and nap-CLA polymeric sheets before and after irradiations show main characteristic bands average at 2920, 2850, 1725 and 1440 cm^{-1} corresponding to ν_{as}(C-H), ν_s(C-H), ν(C=O) and ν(C=C) vibration motions. The absence of ν(NH$_2$) and δ(NH$_2$) of hydrazine group of nap dye at 3354 and 1626 cm^{-1}, respectively, is due to the sharing of –NH$_2$ group of nap dye with –OH of CLA acceptor to associated –$^+$NH$_3$ ammonia group. These results revealed that the composites were just a physical mixture of its constituents and no substitution and elimination reactions were present in the constituents. The infrared spectra of the unirradiated and irradiated composites show that the stability of the free dye and its CT complex was increased by gamma

irradiation with dose of 70 kGy. These results are in good agreement with that of the thermal stability as well as fluorescent efficiency measurements (see Fig. 18).

3.2.2 Electronic spectra studies
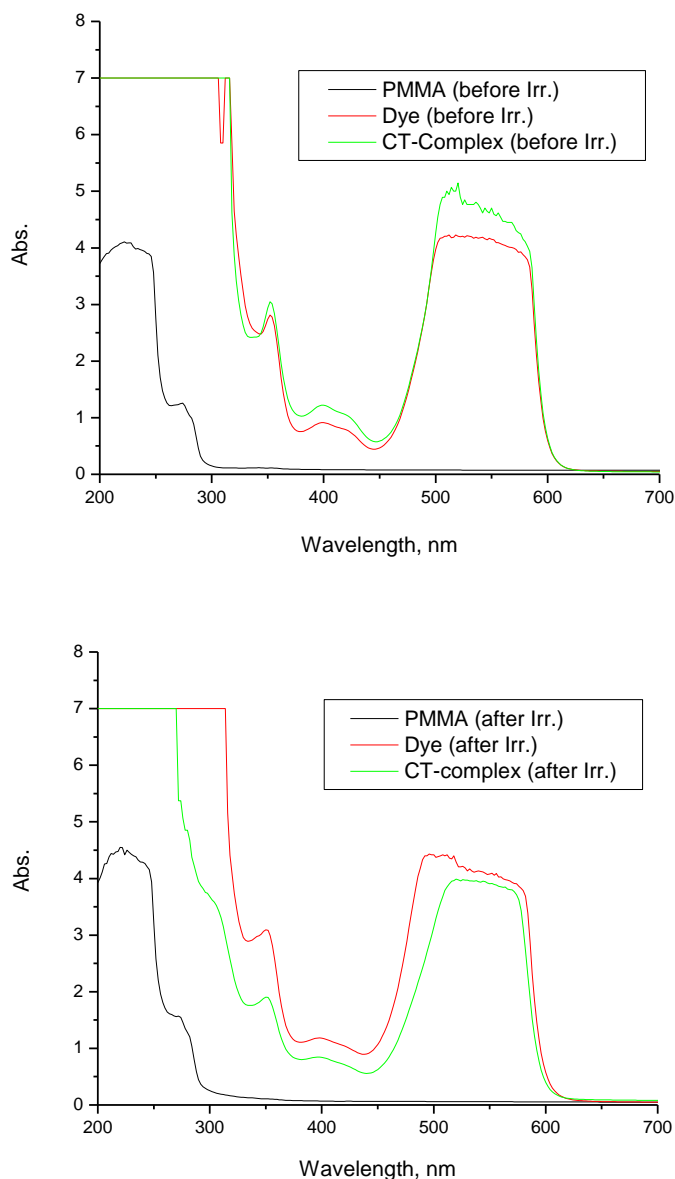
Figure 9. Electronic absorption spectra of PMMA, 2-(4-isobutoxyphenyl)-6-hydrazino-1,8-naphthalimide dye and its charge–transfer complex before and after irradiations.

UV-Vis spectra for polymeric sheets of PMMA (blank), PMMA-nap, PMMA-nap-CLA before and after irradiations are shown in Fig. 9. In this spectra can be seen a characteristic absorption bands of nap-CLA chromophore compound which has two maxima at 330 and 449 nm were bathochromic shifted to 352 and 515 nm. The results show that the charge-transfer complexation increases the stability of nap dye and consequently the absorption from both chromophores increases. All spectra of

pristine and irradiated nap, nap-CLA samples have the similar configuration due to stable bonding between nap dye and chloranilic acid acceptor which already can be used as a model of solar energy source.

Table 4. Optical energy gap determined by the absorption curves of the investigated samples

Sample	E_g (eV) in the transition regions		
	Reg. I	Reg. II	Reg. III
nap (before irradiation)	2.04	3.18	3.40
nap (after irradiation)	2.04	3.10	3.30
nap/CLA (before irradiation)	2.02	3.15	3.37
Nap/CLA (after irradiation)	2.03	3.05	3.19

The absorption mechanism of photons in polymers depends on the transition of charge carriers between valence and conduction bands. The band structure model which is applied in the electronic transition in semiconductors has been used for optical absorption in the organic systems. Thus for a molecular crystal the valence band is formed by the combination of the highest occupied molecular orbital (HOMO; π-orbital) whereas the lowest unoccupied molecular orbital (LUMO; π^*-orbitals) contribute to the conduction band [58,59]. These bands are separated by the band gap (E_g), which can be determined from variation of the optical absorption near the fundamental absorption edge. The relationship between absorption coefficients as a function of the photon energy could be formalized by Bardeen formula [60] which is used in the following form:

$$\alpha h\nu = C(h\nu - E_g)^n \qquad (13)$$

where α is obtained from the formula $\alpha(\nu\square = 2.303A/d$, A is the absorbance, d is the thickness of the polymer film [61]. The constant C is a parameter that depends on the transition probability. The value of the constant n characterizes the direct (n=1/2) and indirect (n=2) allowed transition. By considering the indirect transition (n=2), the $(\alpha h\nu)^{1/2}$ was plotted as a function of hν as shown in Figs. 10 and 11. The optical band gap E_g is determined by extrapolating the linear portion of the obtained curves to zero absorption. All curves of the pristine and irradiated PMMA, nap and nap-CLA samples exhibit three indirect transitions assigned by regions I, II, and III. Such behavior was reported in previous study on γ-irradiated thin films of organic pyronine [62]. Table 4 gives the determined values of the energy gap E_g (see Fig. 10 and 11).
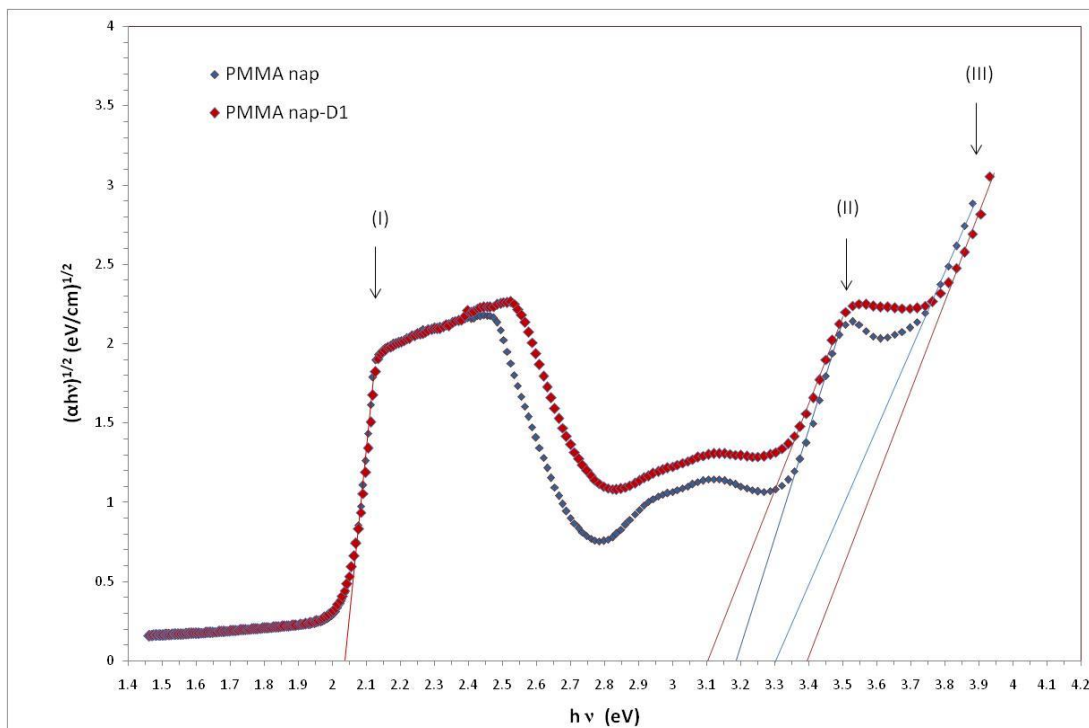
Figure 10. Plots of $(\alpha h\nu)^{1/2}$ as a function of photon energy for the UV absorption of the investigated PMMA(nap) samples: Variation of the optical band gap due to gamma irradiation in the three absorption regions (I, II, III).
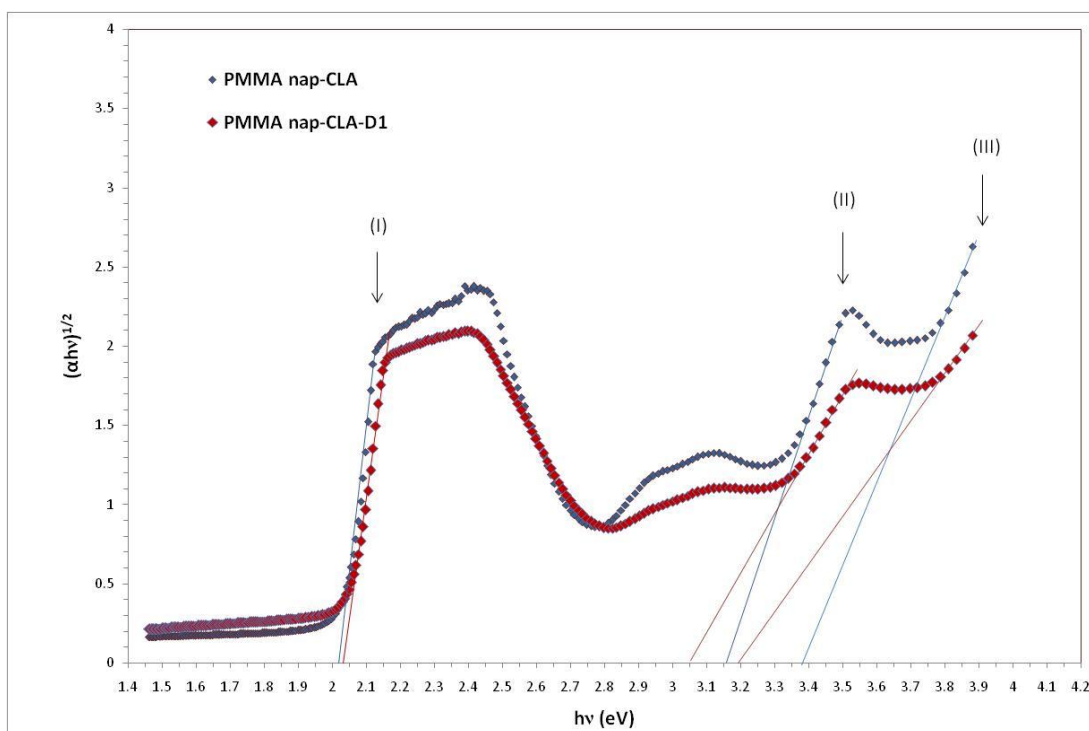
Figure 11. Plots of $(\alpha h\nu)^{1/2}$ as a function of photon energy for the UV absorption of the investigated PMMA(nap-CLA) samples: Variation of the optical band gap due to gamma irradiation in the three absorption regions (I, II, III).

The results indicate that the energy gap was decreased by irradiation in regions II and III which may be attributed to the generation of more localized states by gamma interaction with polymers. At the same time, the probability of transition becomes lower due to increasing of charge carriers on the localized states which require more absorption in this regions and hence reducing the band gap [63].

3.2.3 Positron Annihilation studies
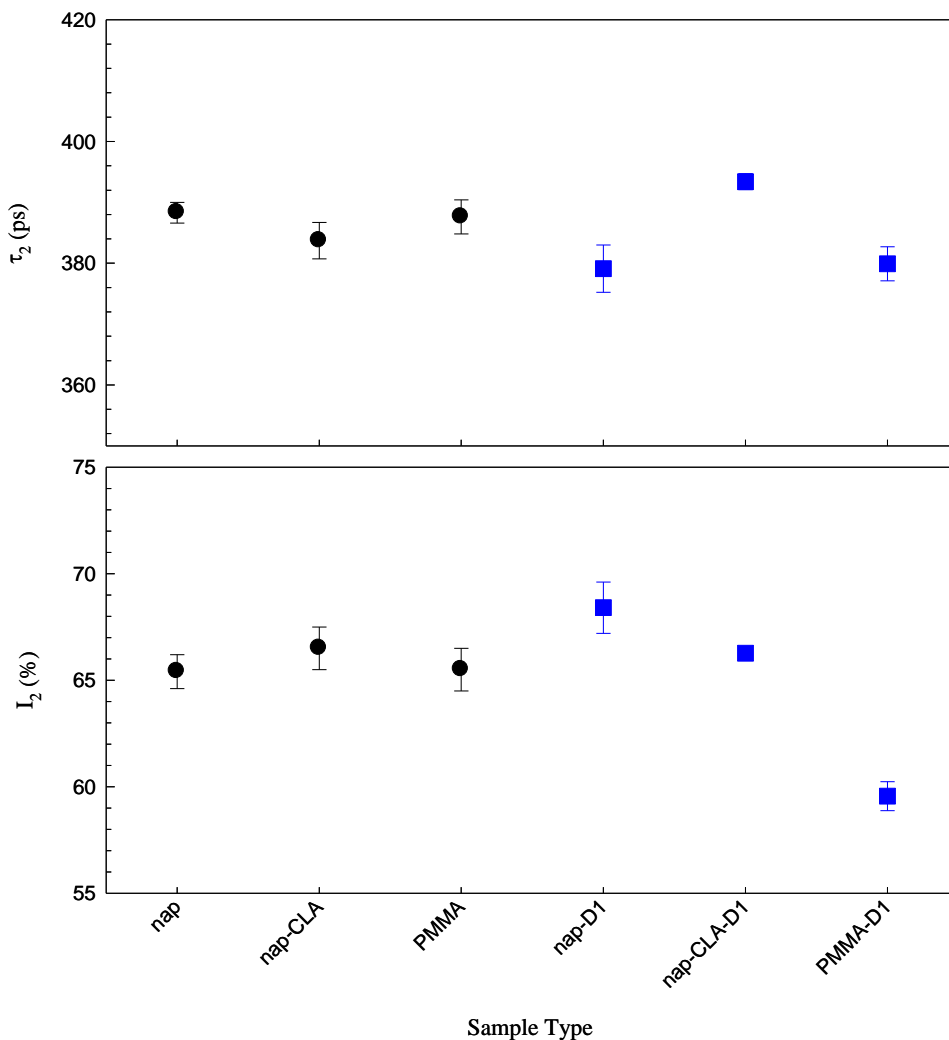
Figure 12. The PAL component τ_2 and its intensity I_2 for the pristine (black closed circle) and irradiated (blue closed square) nap, nap-CLA and PMMA samples.

The lifetime spectra of the pristine and irradiated samples of PMMA polymer, PMMA-nap, PMMA-nap-CLA before and after irradiations were decomposed into three components, τ_1, τ_2 and τ_3. The τ_3 is attributed to pick-off annihilation of the o-Ps in the free volume sites present in the samples of fluorescent dye complex in polymer sheet, which is very sensitive to the microstructural changes. Figures 12, 13 shows the PAL parameters (τ_2, τ_3, I_2 and I_3) for the as-prepared and irradiated samples.

The *o*-Ps lifetime component (τ_3) and its intensity (I_3) of PMMA sample are larger than that values of RMMA-nap and RMMA-nap-CLA samples. This is mainly due to the large size and high concentration of free-volume hole sites and due to the deficiency of delocalized electrons in PMMA polymer sample. The results indicate that the complexation process decreased the values of τ_3 and I_3 due to the closed structure and high electron affinities of PMMA-nap-CLA samples (see Fig. 6). The τ_3 lifetime component ascribed to the annihilation of *o*-Ps indicates that there is one type of vacant due to the homogeneity and crystallinty of the prepared samples. On the other hand, the τ_2 and I_2 are almost constant for all unirradiated samples.
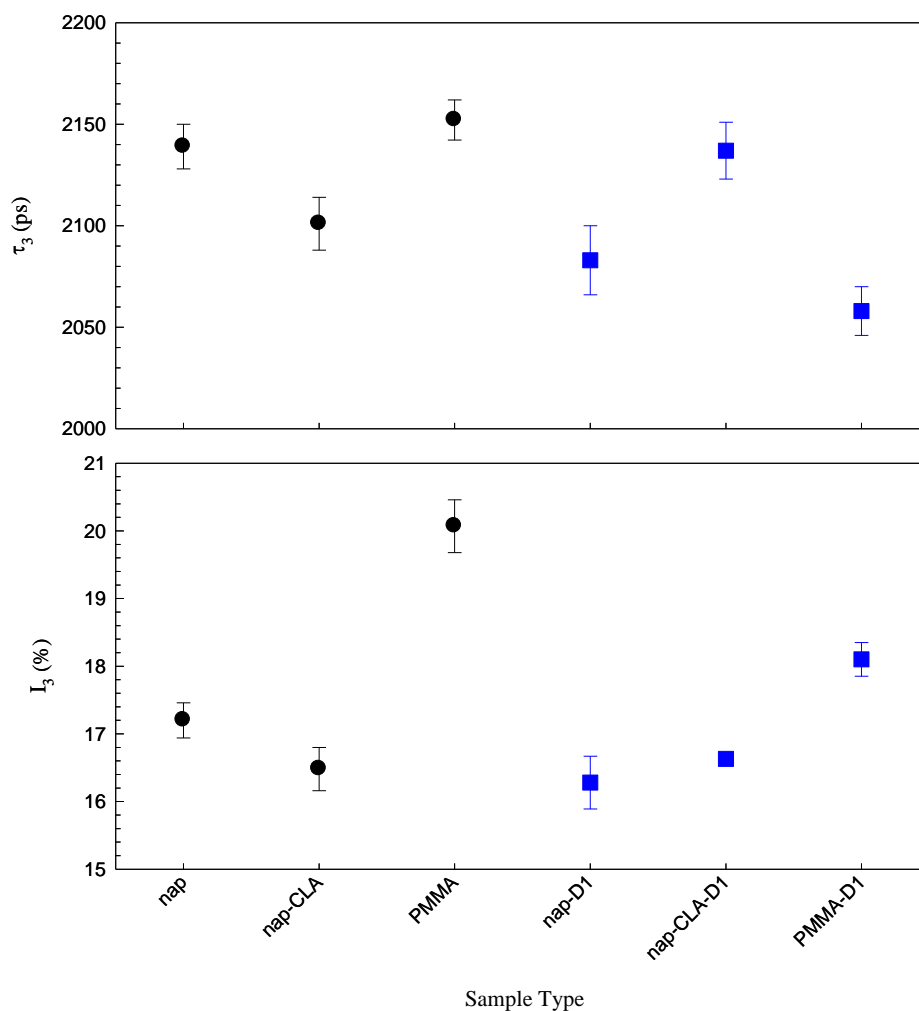
Figure 13. The *o*-Ps lifetime component τ_3 and its intensity I_3 for the pristine (black closed circle) and irradiated (blue closed square) nap, nap-CLA and PMMA samples.

The variation of the mean lifetime for unirradiated samples is shown in Figure 14. The behavior of the τ_m for the unirradiated samples is same as in the case of τ_3 due to the previous reasons. The PMMA polymer and PMMA-nap samples are relatively affected by gamma irradiation of 70 kGy dose as their PAL parameters of irradiated samples are decreased by average values of 3.6 and 7.5%,

respectively, compared with that of unirradiated samples. The effect of gamma irradiation is much strong for PMMA polymer due to the radiation-degradation of the polymers.
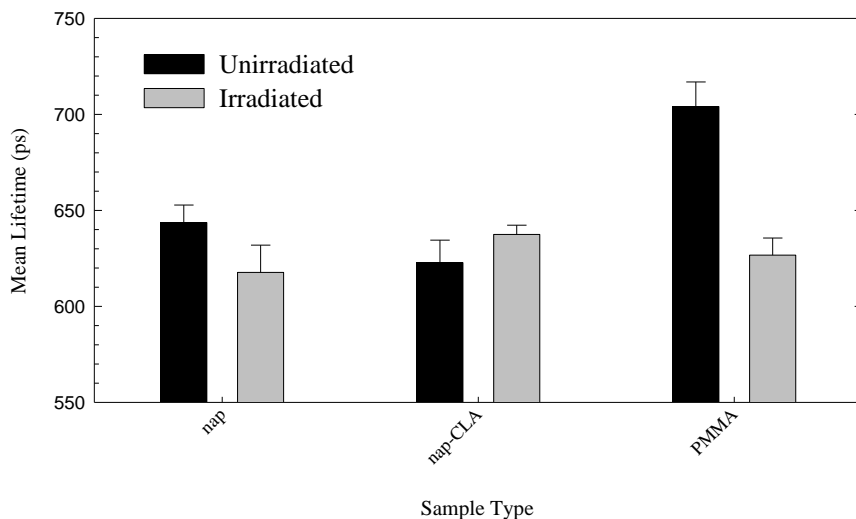
Figure 14. The mean lifetime for the pristine and irradiated nap, nap-CLA and PMMA samples.
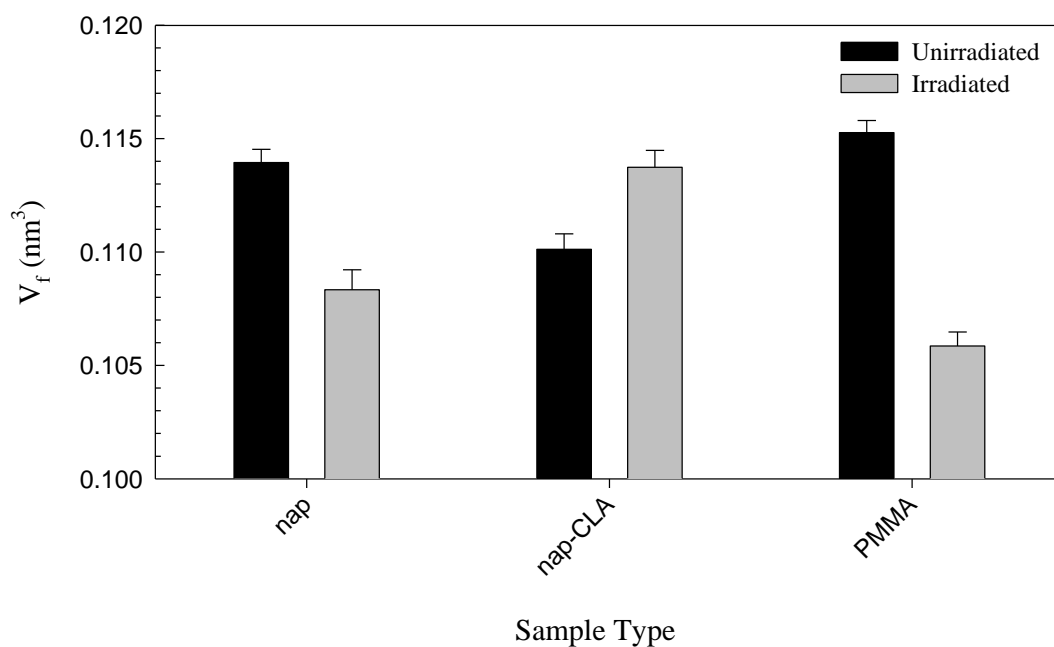
Figure 15. The mean free volume V_f for the pristine and irradiated nap, nap-CLA and PMMA samples.

The results of PAL measurements show that the $[(nap)_2(CLA)]$ CT complex is more stable with gamma irradiation of 70 kGy dose as the PAL parameters of its irradiated sample are slightly increased by an average value of 2.5% compared with that of unirradiated sample. This stability of the CT complex may be due to the stable binding between nap dye and chloranilic acid acceptor. This result is

in good agreement with the results of the measurements of the UV-Vis. and infrared spectra, the thermal stability and the fluorescent efficiency (see section 3.2.4).
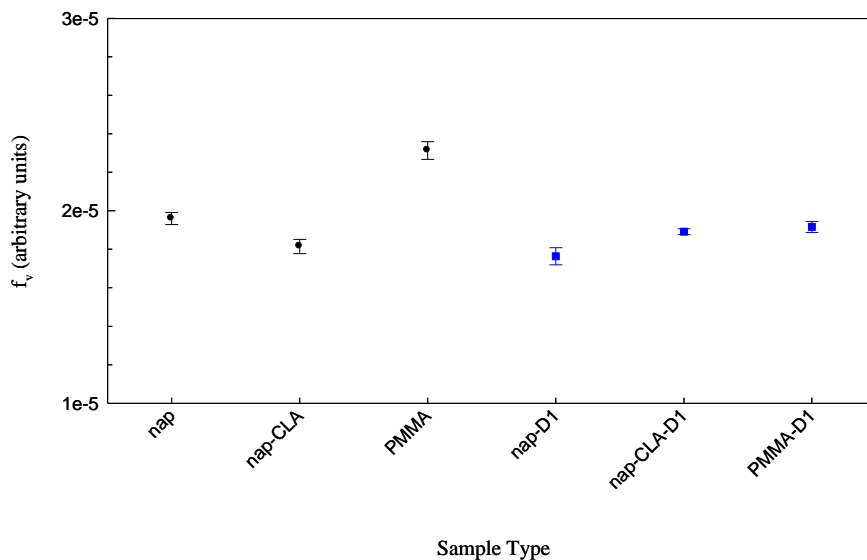
Figure 16. The free volume hole fraction f_v for the pristine (black closed circle) and irradiated (blue closed square) nap, nap-CLA and PMMA samples.
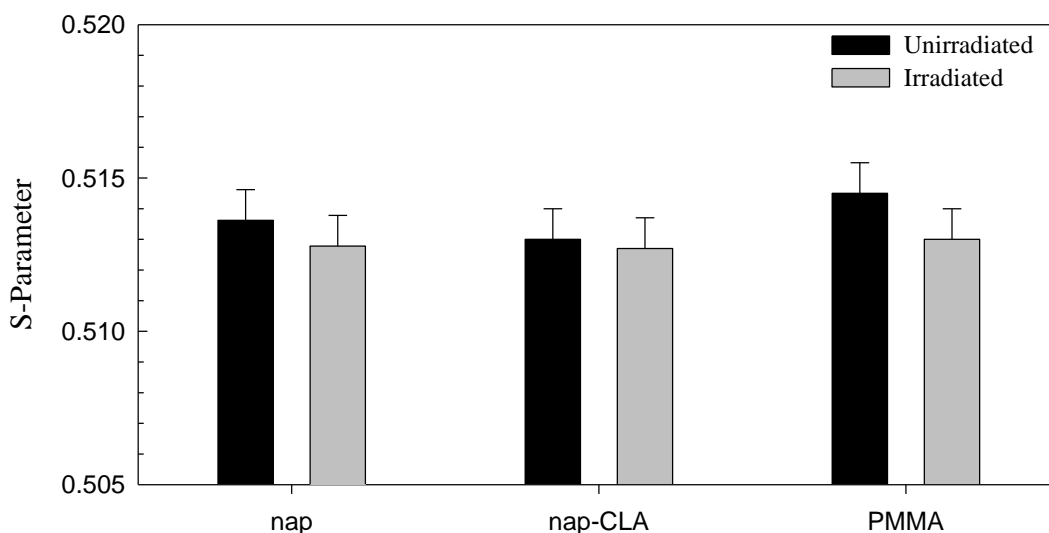
Figure 17. The S-parameter values for the pristine and irradiated nap, nap-CLA and PMMA samples

Figures 15 and 16 show the mean free volume V_f and free volume hole fraction f_v, respectively, for the pristine and irradiated samples. The V_f and f_v values of the PMMA polymer and PMMA-nap samples are decreased, while the value of [(nap)$_2$(CLA)] CT complex is increased by gamma irradiation. On the other hand, the irradiated [(nap)$_2$(CLA)] CT complex show a high V_f value compared with other irradiated samples due to its open chain configuration caused by gamma

irradiation. Therefore, the stability of the CT complex can be explained by the behavior of the V_f and the constant free volume hole fraction for the pristine and irradiated samples (see Figs. 15 and 16). In conclusion, the results of PAL measurements are consistent with the results of other techniques used in this study.

The calculated S–parameter for as-prepared and irradiated PMMA polymer, PMMA-nap and [(nap)$_2$(CLA)] CT complex samples are shown in Fig. 17. The Ps in polymers has been recognized as a unique probe for nano-size free volume holes because of the trapping of Ps in them. In polymers, the S parameter is increased with the increase of free volume size/pore and its concentration [64]. This can be explained as the annihilation with low momentum valence electrons is increased at vacancy sites. The results show that the S–parameter values of the unirradiated samples decrease in the following order PMMA polymer, PMMA-nap and [(nap)$_2$(CLA)] CT complex that is consistent with the previous discussion of results of the PAL measurements. The S-parameter values of pristine and irradiated [(nap)$_2$(CLA)] CT complex sample are almost same and this can explain the stability of this CT complex.

3.2.4 Fluorescence studies
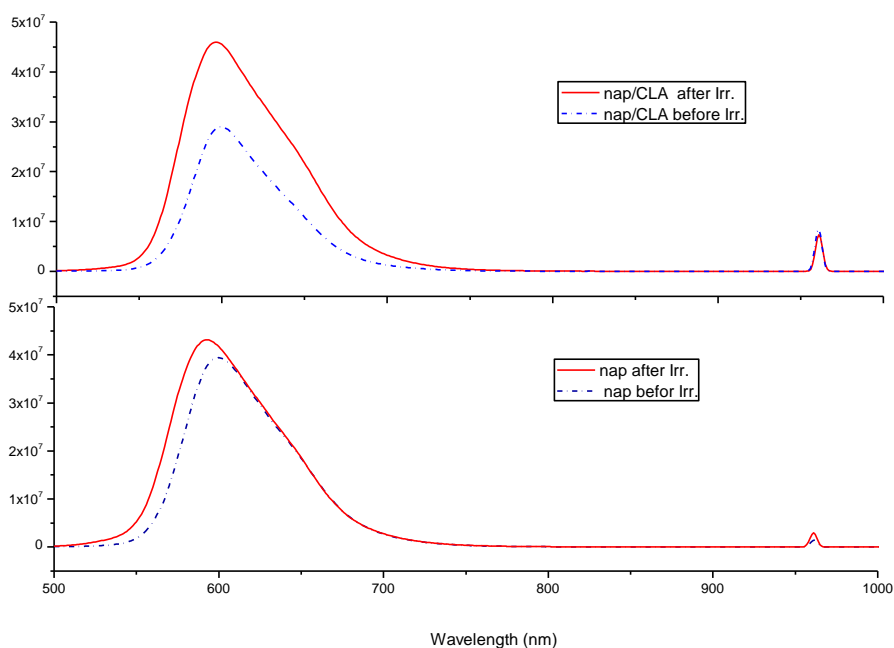
Figure 18. Emission spectra of nap free dye and its chloranilic acid complex in polymeric sheet

We have studied the fluorescence behavior of 2-(4-isobutoxyphenyl)-6-hydrazino-1,8-naphthalimide dye with chloranilic acid in thin film polymer PMMA (Fig. 18). The intensity fluorescence behavior of the dye increased when exposed to irradiation and this could be explained in

terms of the modification of the environment of the dye, polymer and the acceptor with slight change in λ max.

References

1. A.T. Ramaprasad, V. Rao, *Sens Actuators B Chem* 148 (2010) 117.
2. C. Dhand, M. Das, M. Datta, B.D. Malhotra, *Biosens Bioelectron*, 26 (2011) 2811.
3. Q. Wang, J-l. Li, F. Gao, W-S. Li, K-Z. Wu, *New Carbon Mater*, 23 (2008) 275.
4. J.D. Madden, D. Rinderknecht, P.A. Anquetil, I.W. Hunter, *Sens Actuators A Phys*, 133 (2007) 210.
5. G.A. Snook, P. Kao, A.S. Best, *J. Power Sources*, 196 (2011) 1.
6. A.F. Nogueira, C. Longo, M.A. De Paoli, *Coord Chem Rev*, 248(13–14) (2004) 1455.
7. M-C. Choi, Y. Kim, C-S. Ha, *Prog Polym Sci*, 33 (2008) 581.
8. W.A. Gazotti, A.F. Nogueira, E.M. Girotto, L. Micaroni, M. Martini, S. das Neves, M.A. De Paoli, Handbook of Advanced Electronic and Photonic Materials and Devices, H.S. Nalwa, Ed., Academic Press, San Diego, V 10, pp. 54 (2001)
9. H.S. Nalwa, "Optical devices based on conductive polymers" Handbook of advanced electronic and photonic materials and devices, vol 10, Academic Press, San Diego, pp 53–98, 982: *Polym. Bull.* (2013) 70:971–984
10. V.I. Krinichnyi, E.I. Yudanova, *Sol Energy Mater Sol Cells*, 95(8) (2011) 2302.
11. C.L. Chochos, S.A. Choulis, *Prog Polym Sci.*, 36(10) (2011) 1326.
12. Y.-Z. Long, M.M. Li, C. Gu, M. Wan, J-L. Duvail, Z. Liu, Z. Fan, *Prog Polym Sci.*, 36(10) (2011) 1415.
13. W. Schuhmann, R. Lammert, M. Hammerle, H-L. Schmidt, *Biosens Bioelectron*, 6(8) (1991) 689.
14. D. Belo, M. Almeida, *Coord Chem Rev*, 254(13–14) (2010) 1479.
15. W.H. Weber, Lambe, *J. Appl. Opt.*, 15 (1976) 2299.
16. D. Avnir, *Acc. Chem Res.*, 28 (1995) 328.
17. M.S. Refat, S. M. Teleb, I. Grabchev, *Spectrochim Acta*, A61 (2005) 205.
18. M.S. Refat, A. M. El-Didamony, I. Grabchev, *Spectrochim Acta* A, 71(1) (2007) 58.
19. M.S. Refat, S. M. Aqeel, I. Grabchev, *Can. J. Anal. Sci. Spectr.*, 49(4) (2004) 258.
20. Z. Rappoport, *J. Chem. Soc.*, (1963) 4498.
21. Z. Rappoport, A. Horowitz, *J. Chem. Soc.*, (1964) 1348.
22. V.C. Pilho, F. Campos, R. Correa, R. Yunes, R. Nunes, *Quim. Nova* 26 (2003) 230.
23. M. Angadi, D. Gosztola, M. Wasielievski, *J. Appl. Phys.* 118 (1998) 6187.
24. S. Lee, Y. Zu, A. Hermann, Y. Geerts, K. Mullen, A. Bard, *J. Am. Chem. Soc.* 121 (1999) 3513.
25. G. Andric, J. Boas, A. Bond, G. Fallon, K. Ghiggino, C. Hogan, J. Hutchison, M. Lee, S. Langford, J. Pilbrow, G. Troup, C. Woodwar, *Aust. J. Chem.* 57 (2004) 1011.
26. D. Gosztola, P. Niemezyk, W. Svek, A. Lukas, M. Wasielievski, *J. Phys. Chem.* A 104 (2004) 6545.
27. S. Takenaka, K. Yamashita, M. Takagi, Y. Uno, H. Kondo, *Anal. Chem.* 72 (2000) 1334.
28. L. Calcagno, G. Compagnini, and G. Foti, *Nucl. Instrum. Methods* B 65 (1992) 413.
29. R. Mishra, S. P. Tripathy, K. K. Dwivedi, D. T. Khathing, S. Ghosh, M. Muller, and D. Fink, Radiat. *Eff. Defects Solids* 153 (2001) 257.
30. M. Hame, V. Simic, S. Normand, *Reactive & Functional Polymers* 68 (2008) 1671.

31. S. Singh and S. Prasher, *Nucl. Instr. and Meth*. B 222, 518 (2004)
32. D.A. Skoog, Principle of Instrumental Analysis, third ed., Saunders, New York, USA, 1985 (Chapter 7).
33. H.A. Benesi, J.H. Hildebrand, *J. Am. Chem. Soc*. 71 (1949) 2703-2704.
34. R. Abu-Eittah, F. Al-Sugeir, *Can. J. Chem*. 54 (1976) 3705-3712.
35. T. Sharshar, M.L. Hussein, *Nucl. Instr. and Meth*. A 546 (2005) 584.
36. J. Kansy, *Nucl. Instr. Meth*. A 374 (1996) 235.
37. E.A. McGonigle, J.J. Liggat, R.A. Pethrick, S.D. Jenkins, J.H. Daly, D. Hayward, *Polymer*, 42 (2001) 2413.
38. A.O. Porto, G. Goulart Silva, W.F. Magalhaes, *J. Polym. Sci.,* 37 (1999) 219.
39. M. Eldrup, D. Lightbody, J.N. Sherwood, *Chem. Phys*., 63 (1981) 51.
40. K. Ito, Y. Ujihira, T. Yamashita, K. Horie, *J. Polym. Sci*. B 37 (1999) 2634.
41. http://www.ifj.edu.pl/~mdryzek.
42. Y.C. Jean, X. Hong, J. Liu, C.M. Huang, H. Cao, C.Y. Chung, G.H. Dai, K.L. Cheng, Hsinjin Yang, *J. Radioanal. Nucl. Chem*. 210 (1996) 513.
43. M. Schmidtm F.H.J. Maurer, *Polymer* 41 (2000) 8419.
44. A.B.P. Lever, Inorganic Electronic Spectroscopy, second ed., *Elsevier, Amsterdam*, 1985, p. 161.
45. H. Tsubomura, R.P. Lang, *J. Am. Chem. Soc*. 83 (1961) 2085-2092.
46. R. Rathone, S.V. Lindeman, J.K. Kochi, *J. Am. Chem. Soc*. 119 (1997) 9393.
47. G. Aloisi, S. Pignataro, *Journal of the Chemical Society, Faraday Transactions* 69 (1972) 534.
48. G. Aloisi, S. Pignataro, *J. Chem. Soc. Faraday Trans*. 69 (1972) 534.
49. G. Briegleb, Z. Angew. Chem. 72 (1960) 401, Z. *Angew. Chem*. 76 (1964) 326-341.
50. A.N. Martin, J. Swarbrick, A. Cammarata, Physical Pharmacy, 3rd ed., Lee and Febiger, Philadelphia, PA, 1969, p. 344.
51. S.I. Mostafa, *Trans. Met. Chem*. 24(3) (1999) 306.
52. M.S. Refat, A. Elfalaky, E. Elesh, *J. Mol. Struct*. 990 (2011) 217.
53. M. Pandeeswaran, K.P. Elango, *Spectrochim. Acta* A 65 (2006) 1148.
54. K.M. Al-Ahmary, M.M. Habeeb, E.A. Al-Solmy, *J. Mol. Liq*. 162 (2011) 129.
55. A.S. AL-Attas, M.M. Habeeb, D.S. AL-Raimi, *J. Mol. Struct*. 928 (2009) 158.
56. A. Kapor, V. Nikolic, L. Nikolic, M. Stankovic, M. Cakic, L. Stanojevic, *Cent. Eur. J. Chem*., 8(4) (2010) 834.
57. A. W. Coats, J. P. Redfern, *Nature* 201 (1964) 68.
58. M.M. El-Nahhas, Z. El-Gohary, H.S. Soliman, *Opt. Laser Technol*. 35 (2003) 523.
59. J.J. Andre, J. Simon, Molecular Semiconductors, Springer-Verlag, Berlin, 1985, p.73.
60. J. Bardeen, F.J. Slatt, L. Hall, Photo Conductivity Conf. 164, Wiley, New York, 1965.
61. Mark Fox, Optical Properties of Solids, Oxford University Press Inc., New York (2001).
62. H.S. Soliman, A.M.A. El-Barry, S. Yaghmour, T.S. Al-Solami, *J. Alloys Comp*., 481 (2009) 390.
63. S.M. El-Sayed, *Nucl. Instrum. Methods Phys. Res*., B 225 (2004) 535
64. C. He, T. Suzuki, V.P. Shantarovich, N. Djourelov, K. Kondo, Y. Ito, *Chemical Physics* 303 (2004) 219.